Revue Roumaine de Chimie, **2006**, *51*(7-8), 819–826

Dedicated to the memory of
Professor Mircea D. Banciu (1941–2005)

EFFECTS OF AMMONIUM DICHROMATE ADDITIONS ON ELECTROCHEMICAL BEHAVIOUR OF LEAD AND ITS ALLOYS IN H_2SO_4 CONCENTRATED SOLUTIONS

Viorel BRÂNZOI,[a*] Florina BRÂNZOI,[b] Luisa PILAN[a] and Cristina ANGHEL[b]

[a]Department of Physical Chemistry and Electrochemistry, University "Politehnica" of Bucharest, Calea Griviței 132, Bucharest, Roumania, iv_branzoi@chim.upb.ro
[b]Institute of Physical Chemistry Bucharest, Splaiul Independentei 202, Bucharest, Roumania, e-mail: fbrinzoi@chimfiz.icf.ro

Received May 11, 2006

The influence of $(NH_4)_2Cr_2O_7$ additions on the polarization behaviour of $Pb/PbSO_4$ electrode in H_2SO_4 (d=1.25 gcm-^{3}) solution was studied by means of the potentiodynamic method. The lead electrode cycling was carried out within (–1200 to –800 mV) and (+800 to +1600 mV) potential ranges. The ammonium dichromate concentration in the electrolyte was changed from 3.5 ppm to 3000 ppm. The values of the kinetic parameters, determined from the polarization curves, point out the intensification of the anodic and cathodic processes, on addition. Taking into account the shape of the potentiograms, the values of the kinetic parameters from these potentiograms, and the coulometric rations R_1, R_2, R_3 and R_4, a succession of reactions was proposed. Lead and lead-alloys anodes have been show that with increasing anodic polarization, first an insulating layer of $PbSO_4$, then a conductive layer of PbO_2, are successively formed on the electrode. In the PbO_2 potential domain, different crystalline phases (α and β) can be formed, the α phase of PbO_2 being in fact a non-stoichiometric α-PbO_2 layer, with ($1.4<n<2$). The impedance data were consistent with the Pavlov's model of $Pb/PbOn/PbSO_4$ electrode, and the anode behaviour appeared to be essentially determinated by the electrolysis time. It has been shown that the layer growth is first controlled by the solid state diffusion of SO_4^{2-} ions, and then by a chemical step associated with a change in charge carriers taking place at the $PbOn/PbSO_4$ interface.

INTRODUCTION

The lead-antimony alloy of preeutectic composition is generally used for manufacturing the grids of the majority of lead-acid batteries. This alloy has sufficiently high mechanical and casting characteristics, a constant composition in liquid state and a reduced capability to oxidize in manufacturing process. A deficiency of the alloy is the relatively low corrosion resistance, which is limiting the service time of the battery. The increase of the antimony content from the alloy intensifies the corrosion process on one side, and on the other side the antimony has as negative effect the fact that, the Sb is anodically dissolving in solution and it is deposing on active mass of the negative electrode, decreasing the hydrogen evolution overvoltage, which is favoring the increase of the electrode self discharge. For this reason one has passed to the decrease of the antimony percentage in alloy from 8÷12% (how it was at the beginning) down to 5% and even less. In order to improve the quality of the lead-antimony alloys, additions of Ca, Ag, Se, Sn, Te, Cd are used in very small amounts. First, the polarization behaviour of the pure lead has been studied in sulphuric acid solutions with different amounts of ammonium dichromate and then, the polarization behaviours of different lead alloys (Pb + Sb 0,83%; Pb + Sb 1,8%; Pb + Ca 0,086%; Pb + Sb 9,9% + Ag 0,47%; Pb + 0,05% Ca +Sn 0,9%; Pb + 4% Sb + 0,046 % Cu; Pb + 0,138% Ca) were studied. The potential sweep of the working electrode, within given potential ranges, was intended to simulate the processes taking place at the

* Correspondnig author.

positive and negative plates of the lead/acid battery during charge/discharge cycling. The characteristics of the polarization curves (*i.e.*, shape and height and potential range in which peaks appear), as well as the values of the kinetic parameters determined from such curves, enable conclusions to be drawn concerning the electrochemical characteristics of lead and alloys in H_2SO_4 concentrated solutions. Actually, the purpose of this work is to give new information on the effect of different factors, which could improve the formation and functioning technology of the lead –acid battery.

EXPERIMENTAL

Experiments were carried out using the linear sweep voltammetric method with a low potential scan rate (5÷40 mVs^{-1}). The scans were applied by means of a Model 173 Potentiostat-Galvanostat (Princeton Applied Research) provided with a Model 179 Digital Coulometer. The working electrode was made from cylinder of lead or lead alloy with a surface area of 50 mm^2 exposed to the electrolyte solution. The counter electrode was a platinum gauze cylinder and an $Hg/Hg_2SO_4/SO_4^{2-}$ electrode was used as reference. All potentials are reported with regard to this reference electrode. The concentration of the ammonium dichromate, used as additive in the sulphuric acid solution, of $\rho = 1{,}25 gcm^{-3}$, was changed from 3.5 ppm up to 3000 ppm. A number of 20 cycles was carried out for each determination. For electrochemical polarizations, a single compartment cell was used; the lead microelectrode in the middle of the cell was surrounded by a platinum gaze as counter electrode. This arrangement of the two electrodes creates, during the cycling a uniform, intense electric field. A Haber-Luggin capillary was used to assure the binding between the cell compartment and the reference electrode. A sulphuric acid solution of 1,25 gcm^{-3} density was used as basic electrolyte. The temperature was maintained constant, at +20°C, by means of an UM-210 thermostat.

RESULTS AND DISCUSSION

Figure 1 shows the potentiograms of the lead and lead alloys electrodes in sulphuric acid solutions of $\rho = 1{,}25\ gcm^{-3}$ density, obtained as a result of the potential sweep within the -1200mV up to – 800 mV potential range. Analysis of the figure shows the presence of the two current maxima. An oxidation current maximum on the positive-going scan that corresponds to lead dissolution and the formation of a passivating $PbSO_4$ layer. This process is equivalent to the discharge of the negative plate in a lead/acid battery according to the overall equation:

$$Pb \rightarrow Pb^{2+} + 2e^- \rightarrow PbSO_4 + 2H^+ + 2e^- \quad (1)$$

On the reverse potential sweep, a reduction current maximum occurs. This is associated with electroreduction of $PbSO_4$ to metallic lead. The conventional process of reduction takes place, as Popova and Kabanov have shown, by a chemical dissolution of $PbSO_4$ to Pb^{2+} ions, followed by the electroreduction of Pb^{2+} ions to metallic lead, according to the following equations:[1]

$$PbSO_4 + H^+ \rightarrow HSO_4^- + Pb^{2+} \text{(chemical dissolution in acid medium)} \quad (2)$$

$$Pb^{2+} + 2e^- \rightarrow Pb \text{ (electroreduction)} \quad (3)$$

The potential difference between the anodic and cathodic peaks is about 60mV. The height of the cathodic peak is much smaller than that of the anodic peak. Furthermore, a limiting current appears on the cathodic scan. This is due to diffusion control of the reduction process through the semipermeable membrane of $PbSO_4$. It has also been found that a considerable cathodic current is maintained, thus showing that at –1200 mV the reduction of the lead sulphate layer is not fully accomplished. Analysis of Fig. 1 shows that, at the working electrode cycling the peak currents, the average of the anodic and cathodic currents, respectively, is much higher at the first cycle, comparatively with the other cycles. This behaviour can be explained by the fact that, at the first cycle the electrode surface is free of oxides or other compounds, a result of the electrode surface pretreatment before each run; this is resulting in anodic and cathodic processes more intensified than at the other cycles, where the surface is no more completely free. The alloying elements addition in the concentrations mentioned above does not lead to the displacement of the oxidation and reduction peaks; they appear in the same potential ranges as in the case of the pure lead electrode, the parameters which modify being their height, as well as the electricity amounts involved in the anodic and cathodic processes.

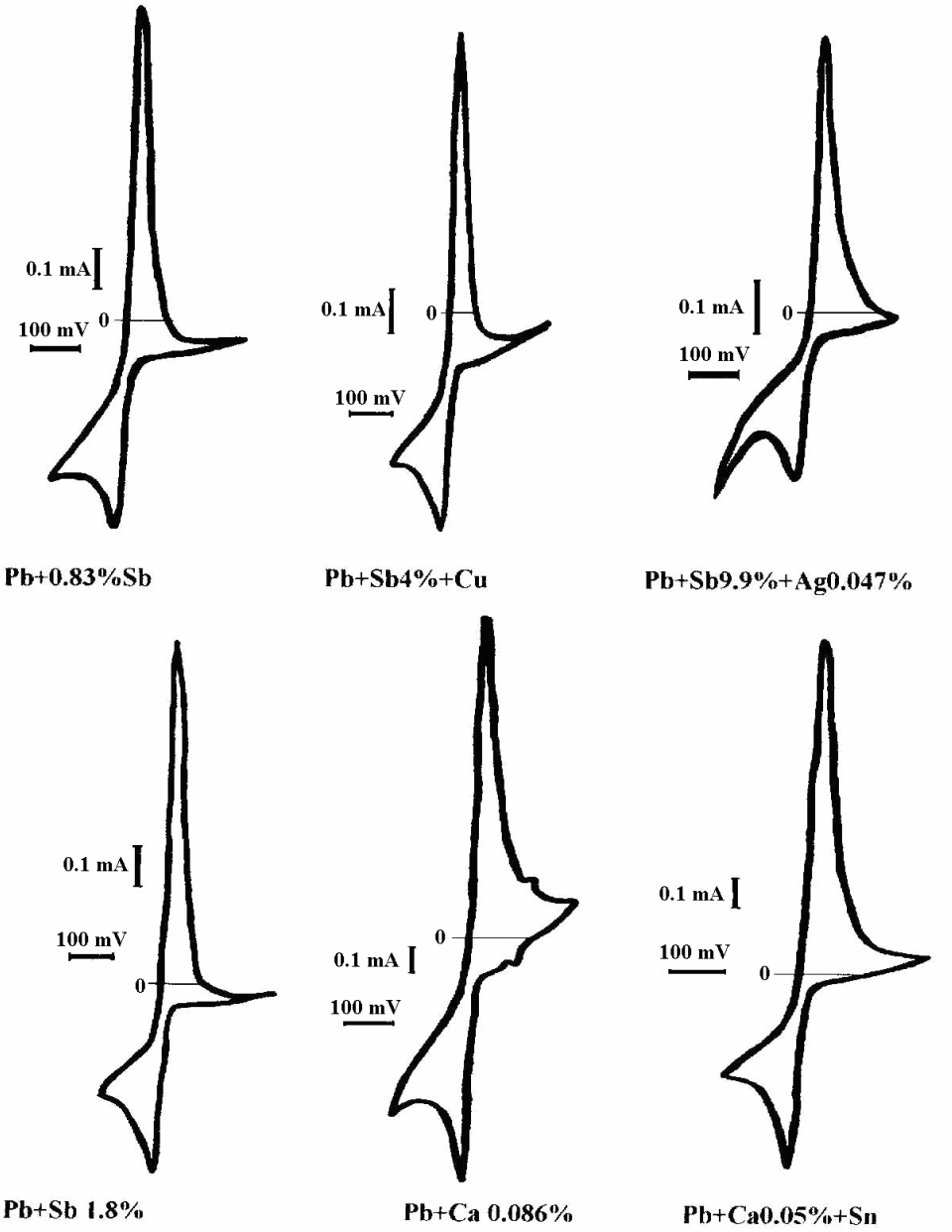

Fig. 1 – The potentiograms obtained at the 20th cycle for lead and lead alloys electrodes in sulphuric acid solutions of ρ = 1,25 gcm^{-3} density, within the –1200mV up to –800mV potential range, with a potential scan rate of 5mVs^{-1}.

In order to better point out these aspects, from the polarization curves, the anodic and cathodic peak currents, as well as the maximum current of the hydrogen evolution corresponding to the potential of –1200 mV have been calculated for the pure lead as well as for the alloys under study – see Tab. 1.

Further on, the influence of the alloying elements on the polarization behaviour of the working electrode was studied, within the (–1200 to 800) mV potential range.

Fig. 1 shows comparatively the potentiograms obtained at the 20th cycle for the pure lead and the lead alloys. Analysis of these potentiograms shows the following: the shape of the polarization curves is the same in all cases; the presence of the alloying elements has led in all cases to the increase of the anodic and cathodic peak currents as well as of the average of the respective currents, which represents an activation of all anodic and cathodic processes.

Table 1

The values of the anodic and cathodic peak currents, as well as the maximum current of the hydrogen evolution within the (–1200 to –800 mV) potential range, in a H_2SO_4 solution (ρ=1,25gcm^{-3}) with a potential scan rate of 5mVs^{-1}

Ipa(mAcm^{-2}) No cycle	Pb+ 0.83%Sb	Pb+0.086% Ca	Pb+Ag0.04 7%+ Sb 9.9%	Pb+0.05%Ca+ 0.9%Sn	Pb+ 4%Sb+ 0.046%Cu	Pb+Sb1.8%	Pb+0.138% Ca
1	3.16	7.61	2.74	-	3.97	5.65	-
5	2.75	4.05	0.9	4.97	2.48	4.53	3.48
10	2.63	3.65	0.61	3.42	1.62	2.9	3.32
15	2.63	3.45	0.43	3.24	1.66	2.83	3.29
20	2.59	3.45	0.37	3.24	1.72	2.97	3.23
Ipc(mA/cm^2) No cycle	Pb+ 0.83%Sb	Pb+ 0.086%Ca	Pb+Ag0.04 7%+ Sb 9.9%	Pb+0.05%Ca+ 0.9%Sn	Pb+ 4%Sb+ 0.046%Cu	Pb+ Sb1.8%	Pb+ 0.138%Ca
1	2.09	5.17	3.92	9.08	4.97	5.38	-
5	1.66	3.85	3.06	4.33	3.97	3.82	2.22
10	1.5	3.10	2.66	2.70	2.42	1.98	1.85
15	1.44	2.82	2.49	2.47	2.52	1.77	1.63
20	1.38	2.64	2.37	2.27	2.15	1.70	1.50
IdegH(mAcm^{-2}) No cycle	Pb+ 0.83%Sb	Pb+ 0.086%Ca	Pb+Ag0.04 7%+ Sb 9.9%	Pb+0.05%Ca+ 0.9%Sn	Pb+ 4%Sb+ 0.046%Cu	Pb+ Sb1.8%	Pb+ 0.138%Ca
1	1.72	2.07	4.58	1.95	2.78	1.55	1.22
5	1.72	2.13	4.25	1.95	1.59	1.41	1.10
10	1.78	2.24	4.17	1.77	1.66	0.96	1.00
15	1.84	1.95	4.17	1.75	1.66	0.99	0.97
20	1.68	1.98	4.25	1.75	1.66	0.99	0.91

A study was made of the polarization behaviour of lead and its alloys in H_2SO_4 of ρ = 1,25 gcm^{-3} density within the potential range of +800mV to +1600mV. Figure 2 shows the voltammograms obtained on the lead and lead-alloys electrodes in above mentioned conditions. Analysis of the Fig.2 shows that the sweep of the working electrode potential within the potential range of (+800 to +1600) mV leads to the appearance of some current maxima. On positive-going scans, a small anodic peak (a shoulder, in fact) occurs within the potential range + 820 to + 940 mV. This represents the formation of basic lead oxides and sulphates. A larger peak is observed at higher potentials and is due to the formation of lead dioxide (α and β modifications). After this peak, oxygen evolution takes place and the current increases sharply. It has been shown that with increasing anodic polarization, first an insulating layer of $PbSO_4$, then a conductive layer of PbO_2 is successively formed on the electrode.[2-14] In the PbO_2 potential domain, different crystalline phases (α and β) can be formed, with the possible existence of amorphous zones.[9,15,16] When the oxidation proceeds through the porous $PbSO_4$ layer, the β-PbO_2 phase is formed at the $PbSO_4$/solution interface by a dissolution-precipitation mechanism.[3,16] The α-PbO_2 layer has been shown to result from the oxidation of PbO in solid state.[3,6,8,9]

Then a PbO sublayer is covered by a non-stoichiometric PbO_n oxide whose stoichiometry coefficient n ($1<n<2$), progressively increases when approaching the oxide/solution interface. The lead oxidation into PbO_n involves both the diffusion oxygen atoms in the anodic layer towards the metal and the migration of oxygen vacancies from the metal towards the solution. When n reaches the critical value of 1,4 the α-PbO_n nucleation begins, involving a change of the tetragonal PbO lattice into orthorombic α-PbO_n.[3] It has been also reported that the PbO_n layer conductivity increases with raising both n value and anodic polarization. In our case, this process of PbO_n to PbO_2 oxidation takes place within the (+1350 to +1500) mV potential range and it is pointed out by the peak (A) appearance. At the reverse potential scan on the descendent anodic curve, a peak (B) corresponding to the reduction of PbO_2 to $PbSO_4$ (of Pb^{4+} to Pb^{2+}) appears. The shape of the two peaks differs appreciably: the cathodic peak for PbO_2 to $PbSO_4$ reduction is very sharp (indicating that the cathodic process is under kinetic control), while the anodic peak for the oxidation of $PbSO_4$ and non-stoichiometric lead oxides and basic lead sulphates is smaller and is spread over a relatively wide potential range, indicating that the anodic process of PbO_2 formation is under diffusion control. From Fig. 2 and Tab. 2, one can see that, the presence of the alloying elements has led in all cases to the increase of the anodic and cathodic peak currents as well as of the average of the respective currents, which represents an activation of all anodic and cathodic process from this potential range (+800 to +1600) mV.

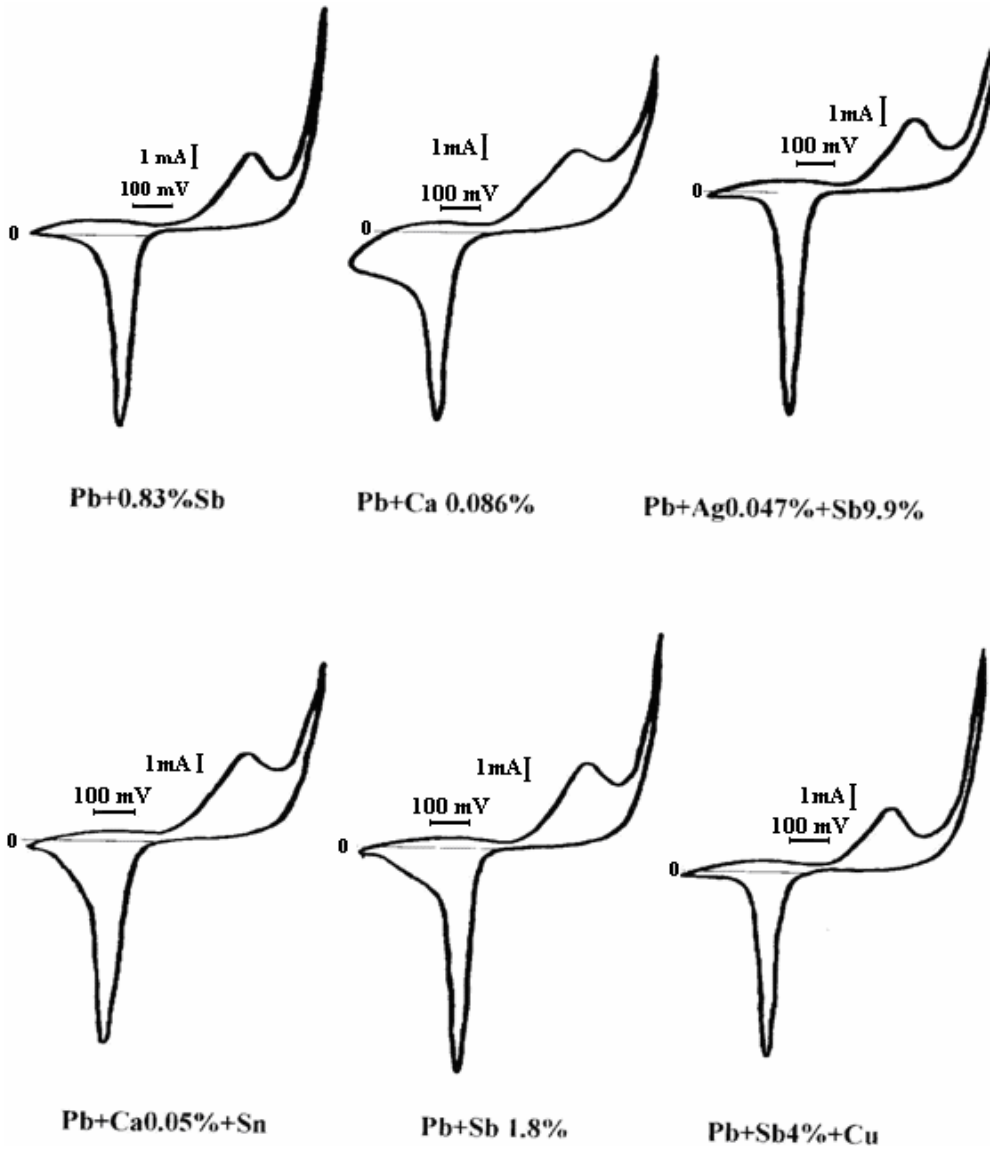

Fig. 2 – The potentiograms obtained at 20th cycle for lead and lead alloys in sulphuric acid solutions of ρ=1,25 gcm^{-3} density, within the +800mV up to +1600mV potential range, with a potential scan rate of 5mVs^{-1}.

Table 2

The values of the anodic and cathodic peak currents, as well as the maximum current of the oxygen evolution corresponding to the potential of +1600mV within the (+800 to +1600 mV) potential range, in a H_2SO_4 solution (ρ=1,25gcm^{-3}) with a potential scan rate of 5mVs^{-1}

Ipa(mAcm^{-2}) No cycle	Pb+ 0.83%Sb	Pb+ 0.086%Ca	Pb+Ag0.047%+ Sb9.9%	Pb+0.05% Ca+0.9%Sn	Pb+ 4%Sb+ 0.046%Cu	Pb+Sb1.8%	Pb+0.138% Ca
1	-	-	-	-	-	-	-
5	5.31	12.64	2.29	11.89	1.59	7.07	8.46
10	6.87	16.95	6.34	17.30	4.97	13.09	11.91
15	9.84	18.39	9.40	21.19	7.62	12.38	14.42
20	12.19	19.54	11.04	23.36	8.78	13.79	15.67
Ipc(mA/cm^2) No cycle	Pb+ 0.83%Sb	Pb+ 0.086%Ca	Pb+Ag0.047%+ Sb 9.9%	Pb+0.05% Ca+ 0.9%Sn	Pb+ 4%Sb+ 0.046%Cu	Pb+ Sb1.8%	Pb+ 0.138%Ca
1	-	-	-	-	-	-	-
5	6.09	30.17	6.87	28.33	5.83	21.22	21.63

Table 2 (continues)

Table 2 (continued)

10	21.56	36.78	20.44	42.38	16.56	36.08	28.21
15	25.62	40.23	26.16	44.77	22.19	32.54	33.54
20	30.62	42.24	30.66	51.25	25.84	35.73	37.00
IdegO(mA/cm^2)	Pb+	Pb+	Pb+Ag0.04	Pb+0.05%	Pb+	Pb+	Pb+
No cycle	0.83%Sb	0.086%Ca	7%+	Ca+0.9%S	4%Sb+	Sb1.8%	0.138%Ca
			Sb9.9%	n	0.046%Cu		
1	4.68	17.24	1.43	14.06	1.12	11.67	34.48
5	7.87	39.94	11.85	35.90	7.48	27.59	35.42
10	10.31	39.66	18.59	14.71	13.58	36.78	35.11
15	10.94	41.67	22.06	45.85	19.54	31.13	38.87
20	14.38	43.10	23.69	46.71	31.47	35.02	39.50

This fact we can explain thus: if the oxidation rate is determined by diffusion of oxygen in the outer (PbO_2) part of the dense layer, the effect alloying agents may be due to an increase in the concentration of oxygen vacancies (i.e. the disorder) in the dioxide lattice. By introducing cations of a lower valence than IV into the PbO_2 lattice the amount of the bound oxygen is reduced and the diffusion of oxygen through the layer is facilitated. For instance, the presence of Sb (III) in the oxide layer might have this kind of influence. On the other hand, if the oxidation rate is determined by diffusion in the inner (PbO) part of the layer, the interpretation of the results is not so straight forward. In this latter case the effect of the alloying agents may be based on an increase in the electronic conductivity of the layer. For instance, the presence of cations with a higher valence than II (Sb(III), Sb(V)) in the layer would lead to an increase in the conductivity of the PbO-like layer. Sb (V) might be bound with oxygen and Pb(II) in the form of lead metantimonate, $PbSb_2O_6$[17]. Also, we have observed that activation energy of the oxide layer growth is lowered by alloying agents. In other words, alloying agents make the energetic barrier for the diffusion of oxygen lower. This can be explained by assuming an increase in the concentration of the oxygen vacancies. In the case of antimonial alloys the activation energy decreases with the antimony content. It is interesting to note that the activation energy for the Pb-Ca-Sn alloy is lower than for the Pb-Ca alloy. This may be connected with the depassivating effect of Sn. At finally, we can conclude that, the effect of alloying elements on the oxidation rate is at least partly based on differences in the microstructure of the metal.

Impedance spectroscopy experiments

Complex plane and corresponding impedance Bode plots for Pb +0,83% Sb in solutions of H_2SO_4 with ρ = 1,25 g/cm^3, at the potential of +1250 mV after different immersion times are shown in Fig. 3. A capacitive semicircle is clearly evident in the complex plane plot, and the polarization resistance was determined from its diameter. As expected, the polarization resistance decreased with immersion time, indicating an increased corrosion rate with immersion time. Plots a, b and c in Fig. 3 consist of a high-frequency capacitive loop and a low-frequency branch, as we can see, in spite of a similar shape, these plots lead to different values for the high-frequency capacitance C and also for the inclination θ of the low-frequency branch. For plot c, the low-frequency impedance is inversely proportional to the square root of frequencies, in conformity with Warburg impedance. This impedance likely corresponds to a solid state diffusion process. On the other hand, the scattered values of C obtained from plots a, b and c are much higher than the capacitance of 0,025 μFcm^{-2}, which can be calculated for a 0,5 μm thick $PbSO_4$ layer of dielectric constant ε_r = 14,3.[18]

Consequently it appears that the values of C reflect a faradic process taking place in the layer and characterized by a poor reproducibility. With increasing electrolysis time, the high frequency capacitive loop progressively disappears and the electrode tends to behave as a dispersive capacitance, as observed on plot c in Fig. 3.

Finally, we can concluded that, the potential domain investigated in the present study, from 0,8V to 1350V, is a transition region corresponding to both the formation of a $PbSO_4$ layer and the coexistence of PbO, PbO_n, α-PbO_2 and β-PbO_2 in the oxide sublayer. Our impedance data and polarization curves obtained in the base electrolyte can be interpreted on the basis of the $PbO/PbO_n/PbSO_4$ electrode, where PbO_n represents a thin oxide sublayer in which various oxides PbO, PbO_n and α-PbO_2, β-PbO_2 can coexist.

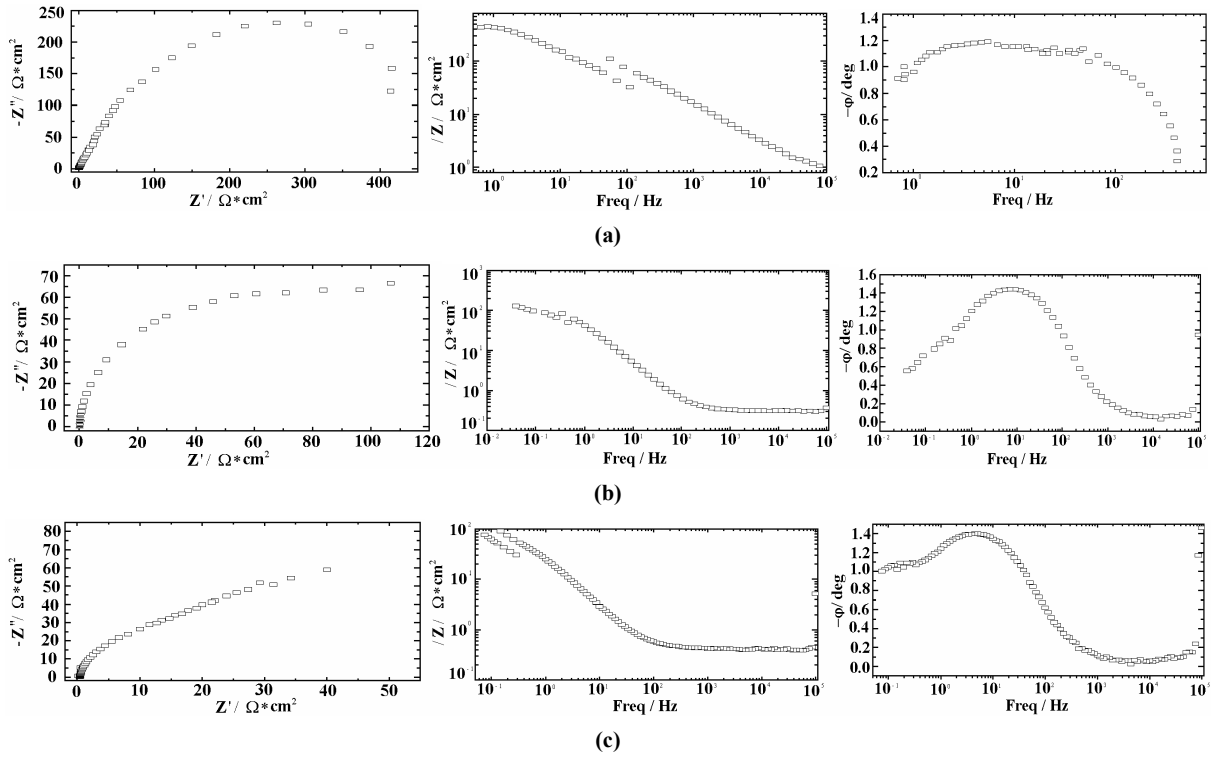

Fig. 3 – Complex plane and Bode plots of the lead alloy Pb 6+0.83%Sb in H_2SO_4 concentrated solutions (ρ=1,25gcm^{-3}) at +1250 mV anodic potential and different immersion times: a) 5min, b) 30min, c) 60min.

Effect of ammonium dichromate

The influence of small additions of ammonium dichromate, $(NH_4)_2Cr_2O_7$, on the polarization behaviour of the lead electrode was studied in H_2SO_4 solutions within +800 to +1600mV potential range. It was found that the additive does not change the shape of the polarization curve, but causes a considerable increase in the height of both the anodic and the cathodic peaks as well as in the amounts of electricity involved in these processes. These features indicate that ammonium dichromate intensifies both processes. It is suggested that the electrode processes occurring in the presence of the dichromate ion during the positive-going scan from +800 to +1600 mV are:

$$2Cr^{6+} + 3Pb \rightarrow 3Pb^{2+} + 2Cr^{3+} \quad (4)$$

(at potentials:+800 to +1200mV)

$$2Cr^{6+} + 3Pb^{2+} \rightarrow 3Pb^{4+} + 2Cr^{3+} \quad (5)$$

(at potentials > +1200 mV)

$$Pb^{2+} \rightarrow Pb^{4+} + 2e^- \quad (6)$$

$$Cr^{3+} - 3e^- \rightarrow Cr^{6+} \quad (7)$$

On the negative going-scan from +1600 to +800 mV, reduction of the formed PbO_2 takes place, *i.e.*,

$$Pb^{4+} + 2e^- \rightarrow Pb^{2+} \quad (8)$$

Taking into account that:

$$Q_a = Q_{PbO_2} + Q_{O_2} = Q_c + Q_{O_2} \quad (9)$$

$$Q_{PbO_2} \text{ (anodically formed)} = Q_{PbO_2} \text{ (cathodically reduced)} = Q_c \quad (10)$$

Hence:

$$Q_{O_2} = Q_a - Q_c \tag{11}$$

the coulometric ratios R_1, R_2, R_3 and R_4 have been calculated as follows:

$$R_1 = \frac{Q_{O_2}}{Q_{O_2}^{\,0}} \times 100 = \frac{Q_a - Q_c}{Q_a^{\,0} - Q_c^{\,0}} \times 100 \tag{12}$$

$$R_2 = \frac{Q_{PbO_2}}{Q_{PbO_2}^{\,0}} \times 100 = \frac{Q_c}{Q_c^{\,0}} \times 100 \tag{13}$$

$$R_3 = \frac{Q_{PbO}}{Q_{O_2}} \times 100 = \frac{Q_c}{Q_a - Q_c} \times 100 \tag{14}$$

$$R_4 = \frac{Q_{PbO_2}}{Q_{total}} \times 100 = \frac{Q_c}{Q_a} \times 100 \tag{15}$$

where the ° superscript refers to H_2SO_4 solution free from $(NH_4)_2Cr_2O_7$. The coulometric ratios (defined by equations 9-15) indicate that, the dichromate anion is accelerating the anodic oxidation of Pb to $PbSO_4$ and PbO and, consequently, it is determining the acceleration of all anodic and cathodic processes, this fact being pointed out by the shape of the obtained voltammograms and by the electrochemical parameters values determined from these ones.

CONCLUSIONS

The suggested mechanism relies on the Pavlov's and Coworkers model, for the electrochemical oxidation of Pb to PbO_2 in H_2SO_4 free of additives;[2,3,5-9]

Based on experimental observations, the formulated mechanism supposes the direct oxidant attack on the metal surface, by the $Cr_2O_7^{2-}$ electrophilic group;

The dichromate anion is accelerating the anodic oxidation of Pb to$PbSO_4$ and PbO and, consequently, it is determining the acceleration of all anodic and cathodic processes;

Our impedance data and polarization curves obtained in the base electrolyte can be interpreted on the basis of the $Pb/PbO_n/PbSO_4$ electrode, where PbO_n represents a thin oxide sublayer in which various oxides PbO, PbO_n and α-PbO_2 can coexist.

REFERENCES

1. T.Y. Popova and B.N. Kabanov, *Zh. Prikl. Kim*, **1959**, *32*, 326.
2. D. Pavlov, S. Zanova and G.Papazov, *J. Electrochem,. Soc*, **1977,** *124*, 1522.
3. D. Pavlov and Z. Dinev, *J. Electrochem. Soc*., **1980**, *127*, 855.
4. S.A. Awad, K.H.M. Kamel and Z.A. Elhady, *Electroanal. Chem. and Interfacial Electrochem.*, **1972**, *34*, 431.
5. T.H.M. Seber and A. M. Shams El Din, *Electrochim. Acta*, **1968**, *13*, 937.
6. D.Pavlov*, Electrochim. Acta*, **1978**, *23*, 815.
7. D.Pavlov, *J. Electroanal.Chem*., **1981**, *118*, 167.
8. D.Pavlov and T. Rogachev*, Electrochim. Acta,* **1978**, *23*, 1237.
9. D.Pavlov, C.N. Poulieff and N. Jordanov, *J.Electrochim Soc*., **1969**, *116*, 316.
10. V. Brânzoi, S. Sternberg and L. Apăteanu, *Rev. Roum. Chim*., **1989**, *34*, 937.
11. J.P. Pohl and W. Schendler, *J. Power Sources*, **1987**, *13*, 297.
12. J.P. Pohl and J. Zschoche, *Dechema-Monogr,* **1987**, *109*, 297.
13. E. Hameenoza*, Electrochim. Acta*, **1989**, *34*, 233.
14. C. Rerolle and R. Wiart, *Electrochim. Acta,* **1996**, *41*, 1063.
15. Y.Yamamoto, K. Fumino, T.Ueda and M.Nambu, *Electrochim. Acta,* **1992**, *37*, 199.
16. J.Burbank, *J. Electrochem. Soc*., **1959**, *106*, 369.
17. D.E. Sweets, *J. Electrochem Society,* **1973**, *120*, 92.
18. C.D. Hodgman, R.C.Weast, R.S. Shankland and S.M. Selby, "Handbook of Chemistry and Physics", The Chemical Rubber Publishing Co. Cleveland, Ohio, 1962, p. 262.